Diffusion of carbon in bcc Fe in the presence of Si

D. Simonovic and C. K. Ande
Materials innovation institute (M2i), Mekelweg 2, 2628 CD Delft, The Netherlands

A. I. Duff, F. Syahputra, and M. H. F. Sluiter
Department of Material Science & Engineering, Delft University of Technology, Mekelweg 2, 2628 CD Delft, The Netherlands
(Received 9 December 2009; published 26 February 2010)

The interaction of interstitial carbon with substitutional silicon and the effect of this interaction on the diffusion of carbon within body-centered-cubic iron, are computed using electronic density-functional theory. Both the activation energy for diffusion and the diffusion prefactor are predicted. Good agreement is found for those cases where a comparison with experimental data is possible.

DOI: 10.1103/PhysRevB.81.054116 PACS number(s): 66.30.J−, 64.75.Nx, 82.20.Db

I. INTRODUCTION

Mass transport through atomic diffusion is the rate limiting step in many processes. Of particular importance is the diffusion of carbon in steel, both in the metallic matrix[1–3] and within precipitated carbide phases[4] as recent computer simulations and experiments indicate. It is known that diffusion of carbon, and other interstitial species, is strongly affected by the presence of other alloying elements.[5–10] Most of our current understanding are derived from sophisticated mechanical spectroscopic measurements, especially those based on Snoek damping, augmented with atomistic modeling using fitted solute-interaction parameters.[11–16] Recently, it has become possible to compute solute-interaction energies, diffusion activation energies, and attempt frequencies from *ab initio* calculations.[1,17–20] This provides a verification of earlier intuitive atomistic models of diffusion and solute-interaction models, and it also provides an opportunity for a deeper understanding of the atomistic processes. Here, our aim is to gain a deeper understanding of the effect of Si on the diffusion of C in ferromagnetic bcc Fe. The wide use of transformation-induced plasticity steels which are often high in Si makes this a problem of practical relevance. Experimentally, Si is known to affect the Snoek damping peak associated with C in bcc Fe (Refs. 8, 13, and 21) and it is also known to influence the precipitation of carbides.[22,23] We will not attempt to simulate the Snoek peaks themselves[12,24,25] although an atomistic understanding of carbon transition rates makes this feasible with high accuracy.[24]

The paper is outlined as follows: first, the individual solute atoms, C and Si, in bcc Fe will be examined through density-functional electronic-structure calculations involving supercells. Second, the energetic effect of bringing C and Si solute atoms in close proximity will be computed. Then, the energy barriers for carbon diffusion in Fe-rich Fe-C and Fe-Si-C are determined through climbing-image-nudged elastic band (CI-NEB) (Refs. 26 and 27) calculations. Once the activation energies and vibrational frequencies in the initial, transition, and final states are known, it is possible to determine transition rates and diffusion parameters through application of transition-state theory.[28] The diffusion of C in the presence of a random solid solution of Si in bcc Fe is modeled through kinetic Monte Carlo (KMC) simulations using the diffusion activation energies and frequency factors from transition-state theory. In the KMC simulations, certain atomic processes can be manually modified so that the consequences of these atomistic processes on the macroscopic diffusion behavior can be readily established.

Thermodynamic considerations

In order to determine whether solute atoms "*X*" occupy interstitial or substitutional sites, it is convenient to define a solute excess energy $\Delta E(X)$ as follows:

$$\Delta E(X) = E(\mathrm{Fe}_n X) - nE(\mathrm{Fe}), \tag{1}$$

where, for reasons of optimal error cancellation, all energies, including the energy per Fe atom, $E(\mathrm{Fe})$, are obtained from supercells with the same dimensions. Here, supercells consisting of $3\times3\times3$ and $4\times4\times4$ bcc cubes were used.

The effective interaction energy J between two solute atoms X and "Y" at a certain distance $\mathbf{R_s}$ from each other may be defined as

$$J^{XY}_{\mathbf{R_s}} = \frac{1}{m}[E(\mathrm{Fe}_n XY, \mathbf{R_s}) - nE(\mathrm{Fe}) - \Delta E(X) - \Delta E(Y)], \tag{2}$$

where s indicates a particular neighbor shell and where the multiplicity m takes care of the fact that the finite size and the periodicity of the cell causes the interaction to occur multiple times in a cell for certain $\mathbf{R_s}$. An example for the $3\times3\times3$ cell is the interaction between a substitutional Si at [000] and an octahedral C at $[\frac{3}{2}00]$, where the C atom has another Si neighbor at [300] so that $m=2$.

Interaction between Si and C atoms causes correlations. Given the rather high solubility of Si in bcc Fe, at low concentrations Si must form a random solid solution in bcc Fe where the individual Si atoms are far apart from each other. Carbon atoms, which diffuse much more easily than Si atoms, see below, will arrange themselves around the Si atoms. In the limit of low Si and C concentrations and at thermodynamic equilibrium, while neglecting the effect of C-C and Si-Si interactions, the probability $f_{\mathbf{R_s}}$ that a C atom is present at a distance $\mathbf{R_s}$ of the Si atom can be expressed as follows:

$$f_{\mathbf{R}_s} = f_\infty \exp\left(\frac{-J_{\mathbf{R}_s}}{k_B T}\right), \tag{3}$$

where we have omitted the superscript "SiC" of J for brevity, and k_B and T represent the Boltzmann constant and the absolute temperature, respectively. Beyond a certain distance $\mathbf{R}_{s_{\max}}$, the Si-C interaction approaches zero, and we assume that the fraction of octahedral positions filled with carbon atoms then takes a constant value of f_∞. The C concentration C_C relative to the bcc lattice positions is then given as

$$C_C = C_{Si} \sum_{s=1,s_{\max}} n_s f_{\mathbf{R}_s} + \left(3 - C_{Si} \sum_{s=1,s_{\max}} n_s\right) f_\infty, \tag{4}$$

where the first sum concerns all the carbon atoms within the interaction range $s_{\max}$ of the Si atom, and where we have accounted for three octahedral positions per atom on the bcc lattice in the second term; C_{Si} is the Si concentration on the bcc lattice sites, e.g., $C_{Si}=1$ means that all Fe atoms have been replaced by Si atoms; and n_s is the number of neighbors in shell s. In practice, the composition is fixed so that the probability of C at octahedral sites beyond the interaction range can be extracted from Eq. (4),

$$f_\infty = \frac{C_C}{C_{Si} \sum_{s=1,s_{\max}} n_s \exp\left(\frac{-J_{\mathbf{R}_s}}{k_B T}\right) + (3 - C_{Si} \sum_{s=1,s_{\max}} n_s)}. \tag{5}$$

In the absence of any interaction between Si and C, all octahedral sites have a probability $f_\infty = C_C/3$ of being occupied by a C atom. As the number of C atoms is constant, segregation of C toward (away from) the Si atom will decrease (increase) f_∞. In the limit of dilute C concentration, we may approximate the chemical potential of C according to the theory of ideal solutions. Moreover, as in equilibrium, the chemical potential μ is constant throughout, we may evaluate the chemical potential far away from any Si atom, which gives in the limit of vanishing carbon concentration,

$$\begin{aligned} \mu_C &= \frac{dF}{dC_C} \\ &= \frac{dF}{df_\infty}\frac{df_\infty}{dC_C} \\ &\approx \mu_C^0 + 3k_B T \ln\left(\frac{f_\infty}{1-f_\infty}\right)\frac{1}{3} \\ &\approx \mu_C^0 + k_B T \ln(f_\infty), \end{aligned} \tag{6}$$

where F is the free energy and μ_C^0 is a reference chemical potential. The equation shows that when f_∞ is lowered, the chemical potential is reduced also.

The diffusion parameter D can be computed through an atomistic simulation by placing a single C atom in a large simulation cell and monitoring its movement through the course of a very large number of jump attempts according to the lattice kinetic Monte Carlo method using the residence time or Bortz-Kalos-Lebowitz algorithm.[29] After a certain time t, the carbon atom has moved a certain distance r away from the original position. Using the theory of random walks, the diffusion parameter is extracted through

$$\langle r^2 \rangle = 6Dt, \tag{7}$$

where the brackets $<$ and $>$ indicate an expectation value, typically obtained by averaging over long-time intervals and repeated simulations. D can oftentimes be expressed in the form of an Arrhenius equation,

$$D = D_0 e^{-\Delta E/k_B T}, \tag{8}$$

where D_0 is known as the frequency prefactor and ΔE is the activation energy for diffusion, below mostly referred to as the energy barrier for diffusion. When Si is present, the interstitial sites in the neighborhood of Si are at higher or lower energy than those at infinite distance as listed in Table I. This means that the beginning and end points of the minimum-energy path are shifted, see Fig. 1. Provided that the energy barriers and attempt frequencies are known for all relevant interstitial jumps, the movement of carbon can then be simulated so that the diffusion of interstitial carbon atoms in the presence of substitutional silicon atoms can be computed through Eq. (7). We assume here that the Si atoms do not diffuse but are statically and randomly distributed in the bcc Fe crystal. This assumption is based on the experimen-

TABLE I. Total energies E, excess solute energies ΔE [see Eq. (1)], and effective Si-C interactions J_{SiC} [see Eq. (2)] as computed *ab initio* in a $3a_{bcc} \times 3a_{bcc} \times 3a_{bcc}$ supercell of Fe as described in the text. Composition indicates which atoms are present in the cell, positions are given in units of the bcc lattice parameter ($a_{bcc}=0.283$ nm).

Composition	Position C (a_{bcc})	Position Si (a_{bcc})	E (eV/cell)	ΔE (eV)	J_{SiC} (eV)
Fe_{54}			−443.304		
$Fe_{53}C$	[0 0 0]		−441.229	−6.134	
$Fe_{54}C$	[½ 0 0]		−451.660	−8.356	
$Fe_{54}C$	[½ ¼ 0]		−450.828	−7.524	
$Fe_{53}Si$		[0 0 0]	−441.623	−6.528	
$Fe_{54}Si$		[½ 0 0]	−444.811	−1.507	
$Fe_{54}Si$		[½ ¼ 0]	−445.033	−1.729	
$Fe_{53}SiC$	[½ 0 0]	[0 0 0]	−449.501		0.478
$Fe_{53}SiC$	[½ ½ 0]	[0 0 0]	−449.229		0.750
$Fe_{53}SiC$	[1 ½ 0]	[0 0 0]	−450.000		−0.021
$Fe_{53}SiC$	[1 ½ ½]	[0 0 0]	−450.036		−0.057
$Fe_{53}SiC$	[1 1 ½]	[0 0 0]	−450.023		−0.044
$Fe_{53}SiC$	[3/2 0 0]	[0 0 0]	−450.182		−0.101
$Fe_{53}SiC$	[3/2 ½ 0]	[0 0 0]	−449.947		0.016
$Fe_{53}SiC$	[3/2 1 0]	[0 0 0]	−450.020		−0.021
$Fe_{53}SiC$	[3/2 1 ½]	[0 0 0]	−450.020		−0.021
$Fe_{53}SiC$	[3/2 1 1]	[0 0 0]	−450.050		−0.035
$Fe_{53}SiC$	[3/2 3/2 0]	[0 0 0]	−450.033		−0.013
$Fe_{53}SiC$	[3/2 3/2 1]	[0 0 0]	−450.044		−0.016
$Fe_{53}SiC$	[½ 0 0]	[∞ ∞ ∞]	−449.979		0

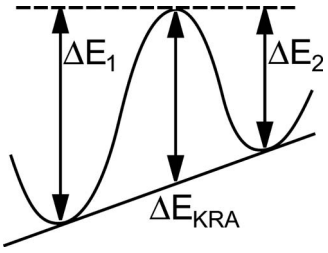

FIG. 1. Schematic view of minimum-energy path between two sites at different energies. Activation energy for a jump from left to right ΔE_1 is not equal to the energy for a jump from right to left ΔE_2. The kinetically resolved activation energy is ΔE_{KRA}.

tally determined C and Si diffusivities in bcc Fe, according to Pascheto and Johari[30] for C the frequency prefactor $D_0=6.61\times10^{-7}$ m^2/s and diffusion activation energy $\Delta E=0.83$ eV whereas according to Bergner *et al.*[31] for Si $D_0=1.7\times10^{-4}$ m^2/s and $\Delta E=2.37$ eV in paramagnetic bcc Fe. The diffusivity of Si is comparable to the self-diffusivity of Fe (Ref. 31) and typically many orders of magnitude slower than the diffusivity of C. Even at $T=1000$ K, the C diffusivity is more than five orders of magnitude greater than that of Si. Therefore, we can safely assume that the Si atoms are statically distributed in the lattice, with the C atoms relatively rapidly moving in the bcc lattice formed by Fe and Si atoms.

An important concept for diffusion between sites with different potential energy is the concept of the kinetically resolved activation barrier (KRA) ΔE_{KRA} (Refs. 32 and 33) displayed in Fig. 1. The KRA energy barrier is the average of the forward and backward diffusion activation energies,

$$\Delta E_{\mathrm{KRA}} = \frac{\Delta E_1 + \Delta E_2}{2}, \tag{9}$$

where $\Delta E_1 - \Delta E_2$ is the energy difference between positions 1 and 2. The energy barrier for C diffusion from a position at a shell s to an octahedral nearest-neighbor position at a shell t is thus according to the KRA approximation,

$$\Delta E_{R_s \to R_t} = \Delta E + \frac{J_{\mathbf{R_t}} - J_{\mathbf{R_s}}}{2}, \tag{10}$$

where ΔE is the activation energy for C diffusion at infinite distance from a Si atom, which takes the value of 0.83 eV. The energy barrier for C diffusion $\Delta E_{R_s \to R_t}$ has not been corrected for temperature effects, such as thermal expansion.

II. CALCULATION METHOD

The electronic calculations used the projector-augmented wave (PAW) method[34] as implemented in the Vienna *ab initio* simulation package[35–37] (VASP). The exchange-correlation potential was of the generalized gradient approximation type as formulated by Perdew and Wang.[38] Integrations in reciprocal space were performed by sampling with Monkhorst-Pack grids; for the 54-atom $3\times3\times3$ bcc cell, we used a grid where six divisions were made along the reciprocals of the **a**, **b**, and **c** axes. Precision was set to "medium." For the 128-atom $4\times4\times4$ bcc cell, a k-point grid was used with four divisions along the reciprocals. In all calculations, the electronic wave functions were expanded in terms of plane waves up to a cutoff kinetic energy of 400 eV. The convergence criteria for energy and force were 0.1 meV and 100 meV/nm, respectively. Structural optimizations were reinitiated at least two times.

The minimum-energy path of carbon atoms between neighboring interstitial sites was computed with the CI-NEB method using the transition-state package developed by Henkelman and Jonsson.[26,27] Images were kept separate using a spring force constant of 500 eV/nm^2.

The diffusion parameter was determined with a random-walk algorithm, a so-called lattice kinetic Monte Carlo simulation, where a single carbon atom was allowed to jump in a cell consisting of $50\times50\times50$ bcc cubes. The bcc lattice positions were all occupied, either with Fe atoms or Si atoms. The Si atoms were randomly distributed in accordance with their atomic concentration. The activation energies for C diffusion were calculated on the basis of the distance to the nearest Si atom using Eq. (10). When the carbon atoms had moved a distance of at least 40 bcc lattice parameters away from the starting position, the elapsed time was determined with the residence time method.[29] This simulation was repeated 20 000 times, each time with a newly generated random distribution of Si atoms, in order to arrive at a suitably averaged diffusion parameter. As only a single carbon atom is present in a supercell with 250 000 bcc positions, there are no interaction effects with other carbon atoms and the computed carbon diffusion parameter pertains to the low carbon-concentration limit. Jumps between neighboring octahedral sites do not exactly correspond to a random walk on a three-dimensional simple cubic lattice because the bcc positions which are filled by Fe atoms are inaccessible so that from any octahedral interstitial position only 4, rather than 6, neighboring positions can be accessed. The attempt frequency has been estimated from the Einstein vibrational frequency ω as follows: $\omega=\sqrt{(k/M)}$, where M is the mass of the carbon atom, 1.994×10^{-26} kg, and k is the spring constant of the carbon atom in the octahedral position, computed from the restoring force on a C atom displaced by 0.1 Å which gives 83.65 N m^{-1}. So that we predict a frequency $\omega=64.76\times10^{12}$ s^{-1}. The bcc lattice parameter has been kept fixed at 0.283 nm. We have not made corrections for thermal expansion, which relative to other errors in these calculations, are believed to be rather minor.

III. RESULTS AND DISCUSSION

Density-functional theory (DFT) results are summarized in Table I. For pure ferromagnetic bcc Fe results concerning lattice parameter ($a_{\mathrm{bcc}}=0.283$ nm) and magnetization per Fe atom ($m_{\mathrm{Fe}}=2.21\mu_B$) are basically identical to those reported in the careful study of Jiang and Carter[17] who used the same software and the same Fe and C PAW potentials as in this study. For the C atom in the octahedral $(\frac{1}{2}00)$ position and the tetrahedral $(\frac{1}{2}\frac{1}{4}0)$ position also, similar energy differences were obtained, the octahedral site in this work being favored by about 0.83 eV. As mentioned by Jiang and Carter,[17] the

tetrahedral position is the saddle point along the minimum-energy path connecting neighboring octahedral positions. Therefore, the energy difference between the octahedral and tetrahedral positions corresponds to the activation energy for diffusion on the octahedral sublattice. The activation energy calculated here, 0.83 eV, compares well with other DFT results 0.90–0.92 eV (Refs. 18 and 19) and 0.86 eV.[17] Our number agrees fortuitously well with the experimentally measured activation energies reported in the literature of 0.87,[39] 0.88,[40] 0.82,[41] and 0.83 eV.[30] More recent Snoek-type measurements have given a similar activation energy of 0.84 eV.[5,23] For completeness, the energy of substitutional C was computed as well. It is found to be about 2.22 eV above that of octahedral C so that under near equilibrium conditions, the occurrence of substitutional C can be ruled out. Another theoretical study[19] reported a similar high energy of 1.97–2.37 eV for substitutional C. The magnetization of supercells Fe_{54} and $Fe_{54}C$, with C in the octahedral interstice, were found to be the same. This indicates that C in low concentrations in the octahedral interstices has little effect of the magnetic properties. Nevertheless, when we define the local moments as the spin density integrated over the Voronoi atomic volumes, we find that the local moments of Fe are clearly affected near the interstitial C atom. The two Fe atoms at the nearest-neighbor positions ($[\frac{1}{2}00]$ in unrelaxed configuration) from the octahedral C atom have local moments that are reduced by about $0.5\mu_B$, the four Fe atoms at the second neighbor ($[\frac{1}{2}\frac{1}{2}0]$ unrelaxed) are unaffected while the eight Fe atoms at the third neighbor ($[1\frac{1}{2}0]$ unrelaxed) have local moments that are enhanced by about $0.14\mu_B$. When C is in the tetragonal interstice, the transition state, the four nearest-neighbor Fe atoms ($[\frac{1}{2}\frac{1}{4}0]$ unrelaxed) are reduced by $0.6\mu_B$ while the four Fe atoms at the second neighbor ($[\frac{3}{4}\frac{1}{2}0]$ unrelaxed) are increased by about $0.2\mu_B$. The net effect of carbon on the magnetization m is nil while it is in the octahedral interstice while the magnetization m is reduced by about $1.5\mu_B$ per carbon atom in the tetrahedral interstitial transition state. This means that the activation energy for carbon diffusion is affected by an applied magnetic field. When the local moments and the applied field are aligned, the activation energy for diffusion is increased by ΔmB, where $\Delta m=1.5\mu_B=87\ \mu\text{eV T}^{-1}$ and where B is the magnetic field. In order to have a 0.1 eV change in the activation energy, a field of 1150 T would be required, which is about one order of magnitude greater than the largest value reported in a nondestructive experiment.[42]

The single Si impurity calculations clearly indicate that Si dissolves substitutionally because it is energetically much more favorable than the octahedral and tetrahedral interstitial positions (see Table I). The Fe-Si nearest-neighbor pairs around the substitutional Si atom are slightly elongated (about 0.4 %), indicating that Si in the metallic environment of Fe is just slightly larger than Fe itself. This immediately indicates that Si is too large to fit in the interstitial positions. Si is indeed experimentally known to be a substitutional alloying element. The bcc lattice parameter of Fe-Si solid solutions is observed to be only weakly dependent on the Si concentration over a large range of compositions, confirming our finding that Si has a size very close to that of the Fe in which it dissolves. Therefore, based on these findings, we have considered the interaction between Si and C in terms of Si-C pairs where the Si atom is always substitutional and the C atom is always in the octahedral interstice.

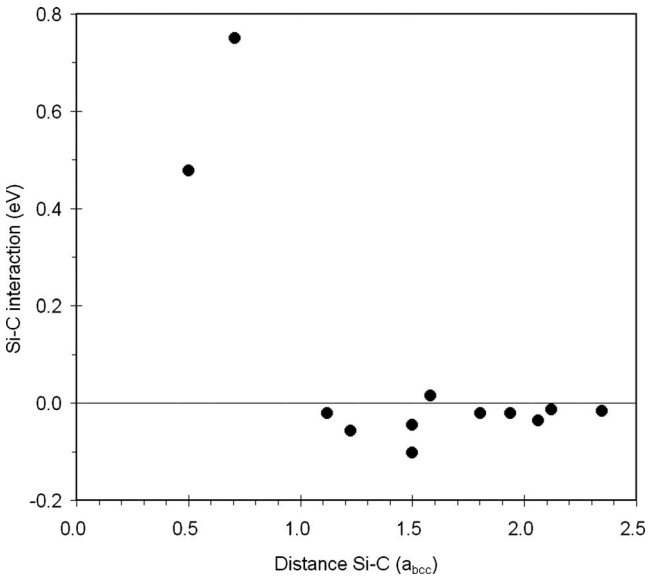

FIG. 2. Computed interaction energy between substitutional Si atom and octahedral (circles) C atom in bcc Fe as a function of distance in units of the bcc lattice parameter.

As apparent from the Table I and Fig. 2, the effective interactions between Si and C are strongly dependent on the distance, they are repulsive at distance less than about a bcc lattice parameter, weakly attractive between 1 and 1.5 times the lattice parameter, and tend to become weak at greater distances. The repulsion at short distances is no surprise; Si is slightly larger than Fe so in its vicinity, there is less room in the interstitial positions. The attractive effective interactions at slightly larger distance might appear surprising but they too can be reasoned. While the first nearest-neighbor Fe-Si pairs are a little elongated, the second-neighbor Fe-Si pairs are a little shortened because the squares formed by first-nearest neighbors are a little expanded. Therefore just beyond a distance of about one bcc lattice parameter, the octahedral interstices are a little less flattened than those in the unperturbed pure Fe crystal structure. Naturally, the C atoms fit a little better here. This attraction is thus an elastic effect. In any case, the attraction is not very strong, at most about 0.10 eV when Si and C are separated by a vector $[\frac{3}{2}00]$. Figure 2 and Table I indicate that the effective interaction is not only a function of distance but also of the particular vector R; the interaction for $[\frac{3}{2}00]$ differs from that for $[11\frac{1}{2}]$ while they are equidistant.

The interaction between Si and C causes variation in the fraction of octahedral interstitial sites that are occupied by carbon, depending on the distance to a Si atom. Beyond the sixth-nearest-neighbor Si-C interactions are negligible so that we may safely assume that the fraction carbon in those shells is the same as at infinite distance from a Si atom. The carbon fraction in various neighbor shells around Si atoms is described by Eqs. (3) and (5) and visualized in Fig. 3. Figure 3 shows that carbon fractions are drawn to the fourth-, fifth-,

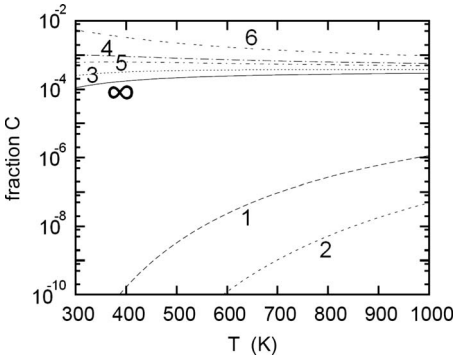

FIG. 3. Carbon fraction in octahedral interstices around a substitutional Si atom as computed according to Eq. (3) for the first six shells around the Si atom and beyond (labeled with ∞), for a composition $Fe_{0.99}Si_{0.01}C_{0.001}$ as a function of temperature.

and sixth-neighbor shells, and are strongly repelled from the first and second shells around Si atoms. Although the attraction is much weaker than the repulsion, on the whole Si atoms attract C, so that the fraction of C at infinite distance from Si is below what it would have been if no Si were present. Therefore, Si effectively decreases the C concentration far away from the Si atoms, and through Eq. (6) it lowers the C chemical potential. This means that C segregation toward Si increases the solubility of C in bcc Fe and suppresses the formation of carbides in bcc Fe.

Figure 4 shows the minimum-energy path for octahedral carbon diffusion in bcc Fe in the absence of Si. In Fig. 4(a), the carbon atom moves between nearest-neighbor octahedral positions such as $[\frac{1}{2}00]$ and $[\frac{1}{2}\frac{1}{2}0]$. The saddle point then occurs at a tetrahedral position ($[\frac{1}{2}\frac{1}{4}0]$) with an activation energy of 0.83 eV. The diffusion pre-exponential factor D_0 was computed also using a dynamical matrix calculation within the 32+1-atom cell,[43] giving $D_0=1.66\times10^{-7}$ m^2 s^{-1}

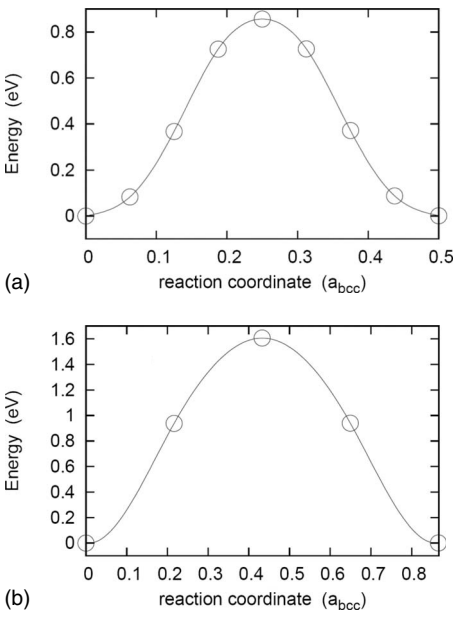

FIG. 4. Minimum energy paths for C diffusion in bcc Fe: (a) C from $[\frac{1}{2}00]$ to $[\frac{1}{2}\frac{1}{2}0]$; (b) C from $[\frac{1}{2}00]$ to $[0\frac{1}{2}\frac{1}{2}]$.

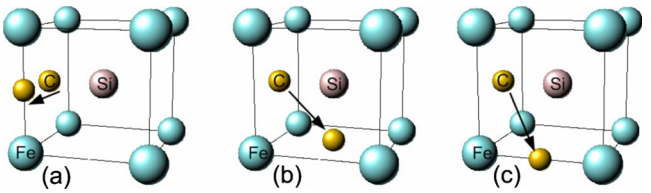

FIG. 5. (Color online) Minimum energy paths for C diffusion in the presence of a single substitutional Si atom in bcc Fe: the Si atom is located at the origin [000], (a) C from $[\frac{1}{2}00]$ to $[\frac{1}{2}\frac{1}{2}0]$; (b) C from $[\frac{1}{2}00]$ to $[0\frac{1}{2}0]$; (c) C from $[\frac{1}{2}00]$ to $[0\frac{1}{2}\frac{1}{2}]$.

for the carbon atom. When the Einstein vibrational frequency of the C atom in its octahedral position is used, i.e., with static neighboring Fe atoms, we find $D_0=\frac{1}{6}(a/2)^2\nu=2.16\times10^{-7}$ m^2 s^{-1}, which is quite close to the full dynamical calculation. A similar calculation by Jiang and Carter[17] involving the local vibrations of the C atom and two nearest-neighbor Fe atoms gave $D_0=1.44\times10^{-7}$ m^2 s^{-1}. The average of the experimentally determined D_0 values[17] is 1.67×10^{-7} m^2 s^{-1}, which agrees well with each of the theoretical numbers. Below, we will discuss the estimate for D_0 from our kinetic Monte Carlo simulations for diffusion.

We have also considered C jumps between non-nearest-neighbor octahedral interstices in bcc Fe without Si. The minimum-energy path between the second-neighbor octahedral sites $[\frac{1}{2}00]$ and $[0\frac{1}{2}0]$ always converged to a path with the octahedral $[\frac{1}{2}\frac{1}{2}0]$ site as intermediary. In other words, the jump between second-nearest-neighbor sites is really two times a nearest-neighbor jump, from $[\frac{1}{2}00]$ to $[\frac{1}{2}\frac{1}{2}0]$ and from $[\frac{1}{2}\frac{1}{2}0]$ to $[0\frac{1}{2}0]$. The minimum-energy path between third-neighbor octahedral sites $[\frac{1}{2}00]$ and $[0\frac{1}{2}\frac{1}{2}]$ could be found however, and it is displayed in Fig. 4(b). It has a very high activation energy of 1.61 eV so that the three nearest-neighbor jumps that connect these sites, e.g., from $[\frac{1}{2}00]$ to $[\frac{1}{2}\frac{1}{2}0]$ next to $[0\frac{1}{2}0]$, and next to $[0\frac{1}{2}\frac{1}{2}]$, have a much greater likelihood of occurring.

In the presence of Si, the nearest-neighbor activation energies are dependent on the proximity of Si. The jumps between second- and third-nearest neighbors, as shown in Figs. 5(b) and 5(c) always reverted to a sequence of nearest-neighbor jumps. The minimum-energy path for the nearest-neighbor jump immediately next to a substitutional Si atom, as shown in Fig. 5(a), is displayed in Fig. 6. For the C jumping from $[\frac{1}{2}00]$ to $[\frac{1}{2}\frac{1}{2}0]$, the barrier does not connect points at equal energy because the $[\frac{1}{2}00]$ site for C is energetically favored over the $[\frac{1}{2}\frac{1}{2}0]$ site by about 0.3 eV, as is apparent from Table I. The activation energy for diffusion is affected also, it is now direction dependent; it is about 0.95 eV from right to left (i.e., from $[\frac{1}{2}\frac{1}{2}0]$ to $[\frac{1}{2}00]$), and about 0.65 eV in the opposite direction. Figure 6 shows all the distinct jumps between octahedral interstices around a single substitutional Si atom in a $3\times3\times3$ bcc cell. For all of these jumps, the KRA (Refs. 32 and 33) takes about the same value. The precise values of ΔE_{KRA} are listed in Table II. Although some variation is seen, particularly at the jumps that are nearest to the Si atom, values are reasonable close to 0.83 eV, the activation energy for C in pure Fe.

In Table III, the computed carbon diffusion coefficient is listed. The values are fortuitously close to those reported in

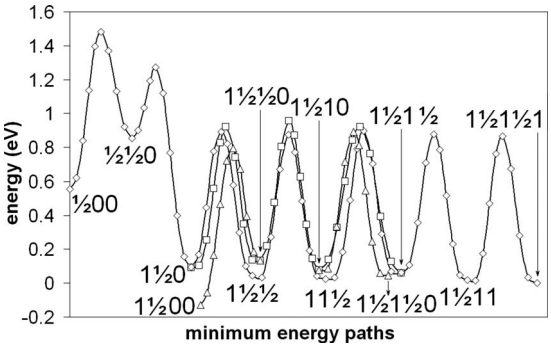

FIG. 6. Carbon diffusion paths in the presence of a single substitutional Si atom in bcc Fe: Si at [000], C jumping between various nearest-neighbor octahedral interstices.

the literature, as Jiang and Carter have found also.[17] D_0 pertaining to carbon diffusivity in the absence of Si can be extracted from the KMC computed diffusion coefficients at 500 and 1000 K. It gives $D_0=1.38\times10^{-7}$ m^2 s^{-1}. This value is two third of the single carbon jump attempt estimate according to $D_0=\frac{1}{6}(a/2)^2\nu$, where the implicit assumption is made that jumps can occur in three dimensions at any octahedral position.[44] Remarkable is the effect of Si on the carbon diffusivity. Especially at low-temperature, carbon diffusivity is reduced by Si, as is illustrated in Fig. 7 where the normalized diffusion coefficient is plotted versus Si concentration. Just 2 at. % Si substitutionally dissolved in bcc Fe reduces the C diffusivity with almost 20% at 500 K and with 8% at 1000 K.

There are two mechanisms by which Si reduces the diffusivity of C: (a) the first- and second-neighbor shells around Si are so high in energy that C is blocked from these sites, this reduces the number of positions through which C can diffuse (labyrinth mechanism); and (b) at slightly greater distances C gets weakly trapped around Si so that it remains immobilized for some time, depending on the temperature (trapping mechanism[14]). The KMC simulations allow to precisely pinpoint the contribution of each mechanism. When the attractive Si-C interactions in the third to sixth shells is set to zero, the C diffusion in Fe with 2 at. % Si is reduced by 12% at 500 K and by 7% at 1000 K. This indicates that at 1000 K, the labyrinth mechanism is the most important. When, instead simulations are repeated whereby the repulsive Si-C interactions in the first and second shells are set to zero, diffusivity in Fe with 2 at. % Si is reduced by 13% at 500 K and by 3.5% at 1000 K. This indicates that at 500 K, the labyrinth and trapping mechanisms contribute about equally but that at 1000 K, the trapping is too weak to play a significant role.

The experience that Si suppresses or retards carbide formation[22,23] now can be understood to have two aspects: (a) by attracting and trapping the C chemical potential is reduced, reducing the driving force for carbide precipitation and (b) by reducing the diffusivity of C, the precipitation of carbides is slowed down. Both effects are sensitive to temperature because Si traps C only weakly. The trapping at a distance of one to one-and-a-half lattice parameters is mostly an elastic effect. Therefore, it is likely that other alloying elements that in the environment of bcc Fe similarly have but

TABLE II. Kinetically resolved activation barriers ΔE_{KRA} (Refs. 32 and 33) as computed with Eq. (9) from the minimum-energy paths (displayed in Fig. 6) for C atoms jumping between nearest-neighbor octahedral interstitial positions labeled "initial" and "final" with a Si atom at a substitutional position [000] in bcc Fe.

Initial a_{bcc}	Final a_{bcc}	ΔE_{KRA} (eV)
$[\frac{1}{2}\ 0\ 0]$	$[\frac{1}{2}\ \frac{1}{2}\ 0]$	0.780
$[\frac{1}{2}\ \frac{1}{2}\ 0]$	$[1\ \frac{1}{2}\ 0]$	0.725
$[1\ \frac{1}{2}\ 0]$	$[1\ \frac{1}{2}\ \frac{1}{2}]$	0.824
$[1\ \frac{1}{2}\ \frac{1}{2}]$	$[1\ 1\ \frac{1}{2}]$	0.838
$[1\ 1\ \frac{1}{2}]$	$[\frac{3}{2}\ 1\ \frac{1}{2}]$	0.854
$[\frac{3}{2}\ 1\ \frac{1}{2}]$	$[\frac{3}{2}\ 1\ 1]$	0.838
$[\frac{3}{2}\ 1\ 1]$	$[\frac{3}{2}\ \frac{3}{2}\ 1]$	0.857
$[1\ \frac{1}{2}\ 0]$	$[\frac{3}{2}\ \frac{1}{2}\ 0]$	0.809
$[\frac{3}{2}\ \frac{1}{2}\ 0]$	$[\frac{3}{2}\ 1\ 0]$	0.850
$[\frac{3}{2}\ 1\ 0]$	$[\frac{3}{2}\ 1\ \frac{1}{2}]$	0.853
$[\frac{3}{2}\ \frac{1}{2}\ 0]$	$[\frac{3}{2}\ 0\ 0]$	0.777
$[\frac{3}{2}\ 1\ 0]$	$[\frac{3}{2}\ \frac{3}{2}\ 0]$	0.831

TABLE III. Simulated carbon diffusivity D (in m^2/s) in bcc Fe as a function of silicon concentration C_{Si} at temperatures T of 500 and 1000 K.

	T	
C_{Si} a/o	500 K	1000 K
0	5.92×10^{-16}	9.00×10^{-12}
0.005	5.33×10^{-16}	8.75×10^{-12}
0.01	5.08×10^{-16}	8.57×10^{-12}
0.015	4.94×10^{-16}	8.35×10^{-12}
0.02	4.83×10^{-16}	8.12×10^{-12}

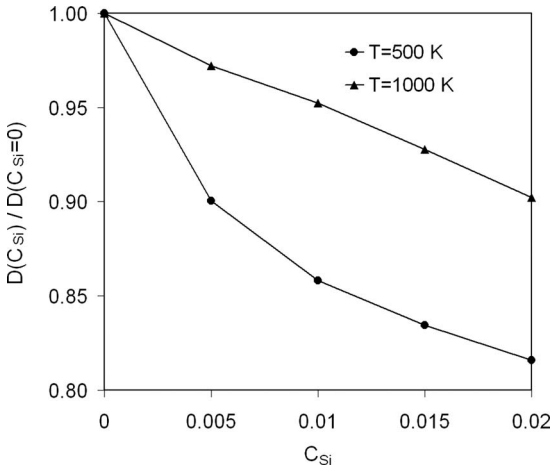

FIG. 7. Predicted C diffusion coefficient in the presence of substitutional Si relative to C diffusion coefficient in the absence of Si, in bcc Fe at temperatures of 500 and 1000 K.

a weak chemical interaction with C, nevertheless can exhibit an analogous trapping effect. Possibly, aluminum acts in a similar fashion. In fact, recent mechanical spectroscopic evidence[5,13] points in this direction. These experiments show that the activation energies for carbon jumps are affected by alloying elements such as Si and Al.[5,13] The effect is found to be stronger when the alloy is cooled slowly, presumably because then the carbon atoms have had time to equilibrate around the Si atoms.[13] The presence of Si gives rise to a broadened activation energy spectrum as compared to the activation energies observed for Fe-C without Si.[13] Our calculations explain this observation because in the presence of Si, a range of activation energies arises from jumps between various neighbor shells around the Si atoms. This resolves a historical puzzle: it has been known that the interaction between Si (Al) and C is repulsive[6] so that C atoms are expected far away from the Si (Al) atoms so that Si (Al) should have a minimal influence of the Snoek peak in bcc Fe-C. However, already the earliest Snoek measurements have pointed to a marked influence of Si and Al.[45–47] Now this apparent contradiction can be understood on the basis of the attractive interactions between Si and C for distances between one and one-and-a-half bcc lattice parameters. The rather small interaction energy between Si and C in bcc Fe is reflected in Snoek measurements. Golovin and Golovina[13] reported that in Fe with 2.94 a/o Si and 0.007 a/o C, only a broadening of the Snoek peak is observed relative to Si-free Fe-C. In contrast, Krishtal[21] reported distinct peaks for C jumps in a pure Fe environment, and for C jumps in the vicinity of a Si atom, the peaks being separated by a mere 25 K in temperature. The difference in activation energies associated with these peaks should be on the order of 0.1 eV or less. On the other hand, our calculations show that jumps between third and more distant shells increase or decrease the activation energies of carbon jumps by up to 0.06 eV (maximum value occurs between sixth and seventh shells) relative to an activation energy of 0.83 eV in the absence of Si. Rather simplistically, we expect therefore to see broadening of the activation energy spectrum as the main effect of alloying with Si although reproducing, and in detail explaining, the Snoek peaks requires a more detailed analysis.[24] We believe that the 0.34 eV binding energy between Si and C as proposed by Walz *et al.*[23] is much too high. The similarity they see with vacancy-C binding (at 0.41 eV) is incorrect because the inward relaxation of the nearest-neighbor Fe atoms around a vacancy is much larger than around a substitutional Si atom. Therefore, the elastic effects that bind a C to a vacancy are much stronger than those that bind C to Si.

In the case of Fe-Al-C, by varying the concentration of Al, the interactions between Al and C, and possibly similarly between Si and C, are concluded to extend up to the third or up to the sixth shell around the Al (Si) atom.[5,13] Here, we find that Si interacts with C up to and including the sixth shell but not beyond that shell.

IV. SUMMARY

It has been shown that the interstitial site preference and the diffusion of C in ferromagnetic bcc Fe can be accurately computed through density-functional electronic-structure calculations. Both the pre-exponential factor and the activation energy for diffusion agree well with consensus experimental assessments. The interaction between Si and C strongly depends on distance, it is strongly repulsive for the first and second shell around the Si atom, weakly attractive in the third up to and including the sixth shell, and essentially vanishing beyond the sixth shell. The weak attraction causes a C-enriched "cloud" around Si atoms at ambient and intermediate temperatures. This reduces the C concentration away from the Si atoms so that in the presence of low Si concentrations, the chemical potential of C is reduced. Therefore, at low concentrations, Si diminishes the thermodynamic driving force for carbide formation. The Si-C interaction is reflected also in the influence of Si on the C diffusivity: (I) at high temperatures of about 1000 K, the strong repulsion between C and Si in the first- and second-neighbor shells dominates. This causes a mild reduction in the C diffusivity because there are fewer diffusion paths as C is blocked from sites very close to Si. (II) At lower temperatures of about 500 K, both the strong repulsion and the weak attraction play an about equal role in reducing the diffusivity of C through both labyrinth mechanism and entrapment of C in the vicinity of Si. At 500 K, 1 a/o of Si in solution may reduce the diffusivity by as much as 14% relative to Si-free bcc Fe. The effect is nonlinear in the composition and appears to saturate for higher Si concentrations.

ACKNOWLEDGMENTS

M. S. gratefully acknowledges H. Numakura and B. J. Thijsse for scientific discussions and I. S. Golovin for making his results available prior to publication and for providing a copy of Ref. 21. D.S., C.A., and M.S. acknowledge support by the Materials innovation institute M2i (www.m2i.nl) in collaboration with the Foundation for Fundamental Research on Matter (FOM) of the Netherlands under Project No. 02EMM032, and by the Materials innovation institute M2i (www.m2i.nl) under Projects No. MC4.05212 and No. MC5.05239, and F. S. thanks Nuffic-Neso (Jakarta) for support.

[1] J. A. Slane, C. Wolverton, and R. Gibala, Metall. Mater. Trans. A **35**, 2239 (2004).

[2] C. S. Becquart, J. M. Raulot, G. Bencteux, C. Domain, M. Perez, S. Garruchet, and H. Nguyen, Comput. Mater. Sci. **40**, 119 (2007).

[3] K. Tapasa, A. V. Barashev, D. J. Bacon, and Yu. N. Osetsky, Acta Mater. **55**, 1 (2007).

[4] A. Schneider and G. Inden, CALPHAD: Comput. Coupling

Phase Diagrams Thermochem. **31**, 141 (2007).
[5] A. Strahl, I. S. Golovin, H. Neuhäuser, S. B. Golovina, T. Pavlova, and H. R. Sinning, Mater. Sci. Eng., A **442**, 128 (2006).
[6] T. Nishizawa, K. Ishida, H. Ohtani, C. Kami, and M. Suwa, Scand. J. Metall. **20**, 62 (1991).
[7] I. S. Golovin, M. S. Blanter, and L. B. Magalas, Defect Diffus. Forum **194-199**, 73 (2001).
[8] D. Ruiz, J. L. Rivera-Tovar, D. Segers, R. E. Vandenberghe, and Y. Houbaert, Mater. Sci. Eng., A **442**, 462 (2006).
[9] I. S. Golovin, S. V. Divinski, J. C. Cizek, I. Prochazka, and F. Stein, Acta Mater. **53**, 2581 (2005).
[10] M. S. Blanter and L. B. Magalas, Scr. Mater. **43**, 435 (2000).
[11] M. Koiwa and H. Numakura, Solid State Phenom. **115**, 37 (2006).
[12] H. Numakura, G. Yotsui, and M. Koiwa, Acta Metall. Mater. **43**, 705 (1995); **43**, 1(E) (1995).
[13] I. S. Golovin and S. B. Golovina, Phys. Met. Metallogr. **102**, 593 (2006).
[14] C. A. Wert and R. C. Frank, Annu. Rev. Mater. Sci. **13**, 139 (1983).
[15] S. Etienne, S. Elkoun, L. David, and L. B. Magalas, Solid State Phenom. **89**, 31 (2003).
[16] H. Saitoh, N. Yoshinaga, and K. Ushioda, Acta Mater. **52**, 1255 (2004).
[17] D. E. Jiang and E. A. Carter, Phys. Rev. B **67**, 214103 (2003).
[18] C. Domain, C. S. Becquart, and J. Foct, Phys. Rev. B **69**, 144112 (2004).
[19] C. Domain, J. Nucl. Mater. **351**, 1 (2006).
[20] D. Simonovic and M. H. F. Sluiter, Phys. Rev. B **79**, 054304 (2009).
[21] Yu. A. Krishtal, Fiz. Met. Metalloved. **19**, 111 (1965); as cited in G. I. Silman and A. A. Zhukov, J. Metal Sci. Heat Treatment **20**, 541 (1978).
[22] A. Okamoto, M. Takahashi, and T. Hino, Trans. Iron Steel Inst. Jpn. **21**, 802 (1981).
[23] F. Walz, T. Wakisaka, and H. Kronmüller, Phys. Status Solidi A **202**, 2667 (2005).
[24] S. Garruchet and M. Perez, Comput. Mater. Sci. **43**, 286 (2008).
[25] J. L. Meijering, Met.: Corros.-Ind. **37**, 107 (1961).
[26] G. Henkelman, B. P. Uberuaga, and H. Jonsson, J. Chem. Phys. **113**, 9901 (2000).
[27] G. Henkelman and H. Jonsson, J. Chem. Phys. **113**, 9978 (2000).
[28] G. H. Vineyard, J. Phys. Chem. Solids **3**, 121 (1957).
[29] A. B. Bortz, M. H. Kalos, and J. L. Lebowitz, J. Comput. Phys. **17**, 10 (1975).
[30] W. Pascheto and G. P. Johari, Metall. Mater. Trans. A **27**, 2461 (1996).
[31] D. Bergner, Y. Khaddour, and S. Lörx, Defect Diffus. Forum **66-69**, 1407 (1989).
[32] A. Van der Ven, G. Ceder, M. Asta, and P. D. Tepesch, Phys. Rev. B **64**, 184307 (2001).
[33] A. Van der Ven and G. Ceder, Phys. Rev. Lett. **94**, 045901 (2005).
[34] P. E. Blöchl, Phys. Rev. B **50**, 17953 (1994).
[35] G. Kresse and J. Furthmüller, Phys. Rev. B **54**, 11169 (1996).
[36] G. Kresse and J. Furthmüller, Comput. Mater. Sci. **6**, 15 (1996).
[37] G. Kresse and D. Joubert, Phys. Rev. B **59**, 1758 (1999).
[38] J. P. Perdew and Y. Wang, Phys. Rev. B **45**, 13244 (1992).
[39] C. A. Wert, Phys. Rev. **79**, 601 (1950).
[40] S. Takaki, J. Fuss, H. Kugler, U. Dedek, and H. Schults, Radiat. Eff. **79**, 87 (1983).
[41] M. Weller, J. Phys. Colloques **46**, C10-7 (1985).
[42] See, e.g., S. A. Crooker and N. Samarth, Appl. Phys. Lett. **90**, 102109 (2007).
[43] This cell is formed by primitive translations $a_{bcc} \times [220]$, $a_{bcc} \times [022]$, and $a_{bcc} \times [202]$.
[44] The third direction is not available for diffusion because the sites in that direction are bcc positions occupied by Fe atoms.
[45] D. A. Leak and G. M. Leak, J. Iron Steel Inst., London **189**, 256 (1958).
[46] F. H. Laxar, J. W. Frame, and D. J. Blickwede, Trans. ASM **53**, 683 (1961).
[47] H. Borchers and W. König, Arch. Eisenhuettenwes. **34**, 453 (1963).